Physically Activated Agricultural Waste Biochars for Production of Pollutant Adsorbents

Despina Vamvuka*, Evangelos Machairas, Stelios Sfakiotakis, Olga Pantelaki

School of Mineral Resources Engineering, Technical University of Crete, Chania, Greece

Abstract: Various nut residues from agricultural production were investigated for their potential to be used as active carbons. Raw materials were pyrolyzed in a fixed bed unit and subsequently gasified by steam or carbon dioxide at different temperatures and duration of heat treatment. Biochars were characterized by physical and chemical analyses with respect to temperature and gasifying agents. Organic and mineral matter, elemental composition, structural characteristics, and surface functional groups were determined. Activation by steam presented a higher reactivity than carbon dioxide, reduced the yield of biochars, consumed more oxygen organic functional groups, favoured pore enlargement at high temperature, and increased the specific surface area (maximum 1257 m^2/g) of pyrolyzed materials by 1.4 to 3.8 fold. Activation by carbon dioxide disrupted the hydrogen char structure, favoured microporosity, and increased the specific surface area (maximum 637 m^2/g) of pyrolyzed materials by 1.8 to 3 fold. Gasified biochars at a high temperature were highly carbonized and exhibited aromatic structures, especially under steam activation.

Key Words: Biochar, Gasification, Steam, Carbon dioxide.

1. INTRODUCTION

Energy and climate crisis across the world, depletion, and the rising cost of fossil fuels demand an increased share of renewable energy in the heating and electricity sector, with minimum environmental impact. Biomass is an important renewable energy source, as it is abundant worldwide, cost-effective and reduces greenhouse gas emissions [1]. Agricultural and agro-industrial wastes, being readily available in large quantities in most countries, offer the remarkable potential for energy recovery as a disposal option, fully meeting the European Union Agricultural and Renewables Policy, relevant to the reduction of biodegradable wastes going to landfills [2].

A thermochemical technology, which converts waste materials into fuels and added-value products, is pyrolysis. Bio-oil and gas generated from this process can provide heat, electricity and/or chemicals. The solid carbonaceous by-product of pyrolysis, biochar, is increasingly gaining attention in recent years, because apart from its potential to be used as fuel, it can contribute to carbon storage and sequestration by remaining in the soil for centuries, it can improve soil properties and fertility as it is rich in nutrients and it can remediate contaminated soil and water bodies by adsorbing heavy metals, polycyclic aromatic hydrocarbons, organic compounds and other

pollutants [3-6]. The potential applications of biochar strongly depend on feedstock types and thermal treatment conditions, especially temperature [3,6-8]. Production from waste biomass is considered a sustainable process, particularly for replacing expensive active carbons.

Active carbons are characterized by a high specific surface area, high porosity and a wide variety of functional groups and pore size distribution, which enable them to adsorb many different molecules. Several reports in the literature have shown that for lignocellulosic biochars, such as corn, barley and rice straws, pine sawdust, poplar, willow and apple branch [1,9,10,11-15], to be effective as active carbons, their porous structure has to be enhanced by activation and their surface and chemical properties modified. Activation can be accomplished by physical or chemical methods. Physical activation takes place at high temperatures (>800°C) in the presence of steam or carbon dioxide, while chemical activation involves the impregnation of biochar with a chemical reagent such as alkali, acids or metal oxides [4,9]. Physical activation is preferred, as being environmentally friendly with lower cost [9,10]. Furthermore, when carbon dioxide from a residual stream is the activation agent, its recycling through this technique gives a potential solution to the greenhouse gas environmental problem [10,16].

Many studies have been carried out using a diverse range of precursor materials of waste biomass, such as agricultural by-products, to assess the benefits of biochars produced from them for the adsorption of

*Address correspondence to this author at the School of Mineral Resources Engineering, Technical University of Crete, Chania, Greece; Email: vamvuka@mred.tuc.gr

hazardous metals, polyaromatic hydrocarbons, and organic pollutants [8,14,17-26]. The physicochemical properties of biochars were determined as a function of the pyrolysis conditions [3,4,6,9,27-29]. Moreover, some studies focused on the enrichment of activated biochar surfaces with hydroxyl or carboxyl groups [5,10], which favour heavy metal adsorption, whereas others focused on increasing the hydrophobicity and polarity of activated biochar [4], which favour adsorption of organic pollutants.

Given the many different biomass types, the multiple production technologies of biochars, and the variety of experimental conditions used, attempts have to be made to characterize each type of source material according to the biochar production and activation method relevant to the targeted application. In this way, a specific type of biomass and its process for conversion to an adsorbent material can be related to the desired physical and chemical properties of biochar produced. Previous investigations on the generation of active carbons from agricultural wastes have examined corn, barley and rice straws, sugarcane bagasse, olive pomace, cotton stalks, cherry and date bones, pistachio, peanut, nutshells etc. [8,9,12,15,20,30-35]. Activation of biochars was conducted by either steam [8,13,32,36-38] or carbon dioxide [10,19,39]. Combined pyrolysis and steam/carbon dioxide gasification have been scarcely documented, as for barley [9] and corn straws [12], focusing mainly on biochar structural characteristics.

Therefore, based on the limited literature data, the objective of this work was to investigate various nut residues from Greece for their potential to be used as active carbons, locally generated and used, thus leading to a sustainable procedure. The availability of these residues has been estimated to about 12000 t/y [40]. Raw materials were pyrolyzed in a fixed bed unit and subsequently gasified by two physical activating agents, steam or carbon dioxide, at different temperatures and duration of heat treatment, without using dangerous substances, as often used by chemical activation methods. Biochars were characterized by physical and chemical analyses with respect to temperature and gasifying agents. Organic and mineral matter, elemental composition, structural characteristics, and surface functional groups were determined. These are key properties for resultant biochars in establishing their suitability to be used as active carbons for the adsorption of heavy metals or organic pollutants. Proper experimental conditions of biochar production and an effective and environmentally friendly activation method are mandatory for industrial processes aiming to produce materials for remediating contaminated soil and wastewaters.

2. MATERIALS AND METHODS

2.1. Raw Materials

The raw materials used for biochar production were agricultural wastes of nut production enterprises in North Greece, namely peach kernels, almond kernels, and walnut husks and kernels. These were ground in a cutting mill and sieved to a final size of < 500 μm. After homogenization and riffling, representative samples were characterized by proximate and ultimate analyses and calorific value, following CEN/TC335 European standards.

2.2. Biochars Production through Pyrolysis Tests

A stainless steel fixed bed reactor (height 14 cm, diameter 7 cm) heated by a furnace was used for the tests. The reactor was charged with about 15 g of biomass sample, which was placed onto a net stainless steel holder. After flushing with pure nitrogen for 30 min at a rate of 150 mL/min, the furnace was set to the selected pyrolysis temperature (700°C or 800°C), at a heating rate of 10°C/min. A Ni-Cr-Ni thermocouple was measuring the temperature inside the reactor (deviation from setpoint ± 5°C). The retention time of pyrolysis was 30 min. Volatile products were passed through iso-propanol cooled by salt-ice baths to collect the condensable fractions. At the end of the experiment, the unit was cooled under nitrogen and the resulting biochar was weighed and stored. The yield of bio-oil was determined by difference from the weight of final liquid condensate and iso-propanol. The yield of gas was calculated by difference.

2.3. Biochars Activation by Steam or Carbon Dioxide through Gasification Tests

Upon completion of pyrolysis, each biochar was loaded into the reactor and heated under nitrogen at the same rate as before, up to the activation temperature (700°C or 800°C, deviation from setpoint ± 5°C). Once the temperature was reached, nitrogen gas was switched to either carbon dioxide with a flow rate of 150 mL/min or to steam by injecting distilled water with a flow rate of 0.5 mL/min using a piston pump. The input of steam at the activation temperature was 2500 mL/min. Activated biochar was held at 700°C or 800°C for 1 hour, after which the furnace was cooled under nitrogen.

2.4. Physical and Chemical Characterization of Biochars

Both pyrolyzed and steam/carbon dioxide activated biochars were characterized by proximate analysis, ultimate analysis, and calorific value, following the European standards CEN/TC335.

Specific surface area, pore volume, and pore size were determined according to the BET method from liquid nitrogen adsorption at 77 °K, using a Quantachrome model Nova 2200 automatic volumetric apparatus. Prior to each measurement, the samples were out-gassed overnight at 150°C under a vacuum of 10^{-6} torr.

The chemical functional groups of biochar samples were identified using a Perkin-Elmer Spectrum 1000 spectrophotometer. Each sample was mixed with KBr at a ratio of 1/100 w/w and pressed into a pellet. Fourier Transform Infrared (FTIR) spectra were recorded in the range 4000-400 cm^{-1} wavenumber at a resolution of 4 cm^{-1}.

3. RESULTS AND DISCUSSION

3.1. Yield of Pyrolysis and Gasification Products

Proximate and ultimate analysis of raw materials is represented in Table **1**. Volatile matter content was high, ranging between 73% and 77%, while ash content was low, i.e., 0.4-2.8%. Elemental concentration was similar for all samples, with almond kernels presenting the highest carbon and lowest oxygen contents. The percentage of nitrogen was low, whereas that of sulfur was undetectable.

Table **2** summarizes the yield of products of pyrolysis under nitrogen and steam or carbon dioxide activation as a function of temperature, while Figure **1** compares the yield of biochars of both pyrolysis and gasification at 700°C. As can be observed, with an increase in activation temperature, biochar yield decreased, and the proportion of gas increased at the expense of that of bio-oil. This increase of non-condensable gases with temperature was due to enhanced biomass decomposition and secondary cracking of volatiles. Previous work in our lab [41] has shown that the higher heating value of pyrolysis gases and bio-oil varies between 11-15 MJ/m^3 and 20-40 MJ/kg, respectively, which is in excess of the energy requirements of pyrolysis units [42]. Furthermore, it can be noticed that the combined pyrolysis-steam or – carbon dioxide gasification led to the production of less biochar with respect to pyrolysis only and more syngas. During steam gasification, the char was converted to CO and H_2 through equation (1), as well as to some CO_2 through the water gas shift reaction, equation (2). During carbon dioxide gasification, the char was principally oxidized to CO, equation (3), while CO_2 could also react with H_2 through the reverse water gas shift reaction to produce more CO and H_2O:

$$C + H_2O \rightarrow CO + H_2 \tag{1}$$
$$CO + H_2O \rightarrow CO_2 + H_2 \tag{2}$$
$$C + CO_2 \rightarrow CO \tag{3}$$

Table 1:   Proximate and Ultimate Analyses of Materials (% dry weight)

Sample	Volatile Matter	Fixed Carbon	Ash	C	H	N	O	S
Peach kernels (PEK)	76.3	23.1	0.6	49.3	6.0	1.2	42.9	-
Almond kernels (ALK)	73.0	26.6	0.4	53.6	6.2	0.4	39.4	-
Walnut husks (WAH)	76.8	20.4	2.8	47.1	6.0	1.0	43.1	-

Table 2:   Yields of Pyrolysis and Gasification Products (% dry weight)

Sample	Temperature (°C)	Biochar			Biooil			Gas		
		N_2	H_2O_v	CO_2	N_2	H_2O_v	CO_2	N_2	H_2O_v	CO_2
PEK	700	29.2	21.5	26.8	43.9	43.9	44.0	26.9	34.6	29.2
	800	27.6	16.4	24.2	33.2	33.2	33.2	39.2	50.4	42.6
ALK	700	29.1	20.8	25.1	36.2	36.2	37.5	34.7	43.0	37.4
	800	19.2	1.7	19.9	36.8	41.7	45.0	44.0	56.6	35.1
WAH	700	25.0	15.9	19.6	44.7	44.7	45.0	30.3	39.4	35.4
	800	24.6	3.3	18.7	42.6	42.5	42.6	32.8	54.2	38.7

Gasification efficiency was much higher in the presence of steam, so that biochar yield dropped to 16-21% as compared to carbon dioxide activation (20-27%), as ure **1** clearly shows. Contrary, gaseous products under steam or carbon dioxide activation increased by 20-40% and 8-15%, respectively, at 800°C. The reasons for the higher reactivity of steam are explained in the sections to follow.
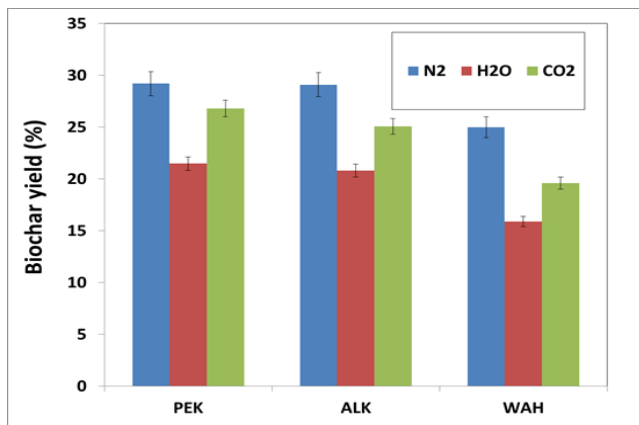

Figure 1: Yield of biochar for pyrolysis and gasification at 700°C.

3.2. Proximate and Elemental Composition of Pyrolyzed and Activated Biochars

The proximate and elemental analysis of biochars pyrolyzed in nitrogen and those activated with steam or carbon dioxide are shown in Table **3**. As can be seen, a higher pyrolysis temperature, from 700°C to 800°C, resulted in an increase in carbon density of biochars and a small enrichment in minerals. On the other hand, the concentrations of hydrogen and oxygen were significantly reduced at the higher temperature, in accordance with previous findings [3,18,19], due to cleavage of weaker bonds, associated mainly with dehydration-decarboxylation reactions. The lower H/C and O/C molar ratios at 800°C indicate the development of more carbonaceous and aromatic structures with greater stability. A greater extent of carbonization occurred for the walnut husks sample.

Moreover, Table **3** shows that gasification of pyrolyzed biochars consumed fixed carbon, further increasing the ash content of biochars. Hydrogen and oxygen decreased sharply upon activation with steam or carbon dioxide, revealing the formation of hydrogenated and oxygenated compounds in the syngas and bio-oil, whereas nitrogen was eliminated from biochars and was mainly transferred to the gas phase. The lower oxygen concentration of steam-activated chars, in comparison to those activated by carbon dioxide, suggests that the oxygen organic functional groups reacted more easily under steam atmosphere. However, carbon dioxide agent disrupted the hydrogen char structure promoting cracking of benzene rings and fracturing of hydroxyl, methyl and methylene groups [11], thus leading to a very low hydrogen concentration of biochars. Figure **2** clearly illustrates that the dry ash-free carbon content of pyrolyzed biochars decreased during gasification with steam or carbon dioxide.
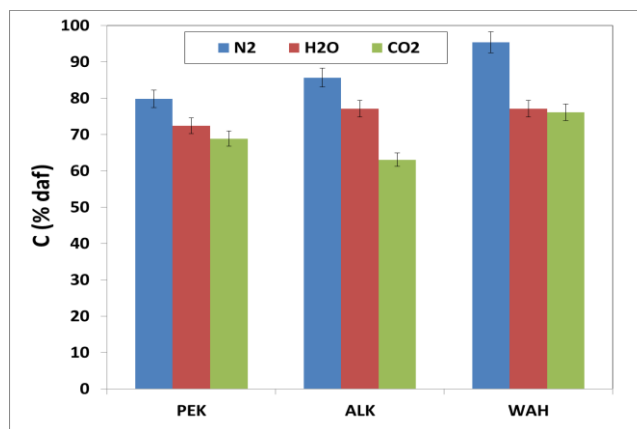

Figure 2: Dry ash free carbon of pyrolyzed and gasified biochars at 800°C.

Table 3: Proximate and Ultimate Analyses of Pyrolyzed and Gasified Biochars (% dry weight)

Sample	Activation	Organic Matter	Ash	C	H	N	O	H/C	O/C
PEK	N_2 (700/800)	98.0/97.8	2.0/2.2	69.9/78.1	2.2/0.8	1.1/0.8	24.8/18.1	0.38/0.12	0.27/0.17
	H_2O_v (800)	95.2	4.8	68.9	1.6	-	24.6	0.28	0.27
	CO_2 (800)	98.0	2.0	67.5	0.7	-	29.8	0.12	0.33
ALK	N_2 (700/800)	98.7/98.6	1.3/1.4	83.8/84.5	1.5/1.3	1.0/1.0	12.4/11.8	0.21/0.18	0.11/0.10
	H_2O_v (800)	85.0	15.0	65.5	1.1	-	18.3	0.20	0.21
	CO_2 (800)	98.0	2.0	61.8	0.8	-	35.4	0.15	0.43
WAH	N_2 (700/800)	89.9/88.6	10.1/11.4	83.5/84.6	1.5/1.4	0.7/0.7	4.2/1.9	0.21/0.19	0.04/0.02
	H_2O_v (800)	76.3	23.7	58.8	1.2	-	16.3	0.24	0.20
	CO_2 (800)	86.5	13.5	69.3	0.6	-	16.6	0.10	0.18

Table 4:   Structural Characteristics of Pyrolyzed and Gasified Biochars

Sample	Temperature (°C)	Activation Gas	Specific Surface Area (m²/g)	Micropore Volumex10² (cm³/g)	Average Pore Size (A)
PEK	700	N_2	348.9	21.0	24.0
		H_2O_v	475.3	21.9	22.2
	800	N_2	305.2	19.0	23.0
		H_2O_v	778.0	38.9	23.9
		CO_2	531.0	24.7	22.3
ALK	700	N_2	172.7	11.5	27.0
		H_2O_v	654.6	33.5	24.6
	800	N_2	202.6	24.5	31.0
		H_2O_v	1256.8	74.8	28.6
		CO_2	607.6	29.9	23.6
WAH	700	N_2	280.7	16.2	23.0
		H_2O_v	647.3	40.6	30.1
	800	N_2	285.8	18.1	24.0
		H_2O_v	692.8	45.1	31.3
		CO_2	637.0	31.8	24.0

3.3. Structural Characteristics of Pyrolyzed and Activated Biochars

The specific surface area is closely associated with pore volume and size and reflects the adsorption capacity of biochars. Table **4** includes the structural characteristics of biochars studied, which were produced after pyrolysis with nitrogen and subsequent activation with steam or carbon dioxide, as a function of temperature. As can be noticed, a greater release of volatiles with temperature from almond kernels and walnut husks elevated the microporosity and surface area up to 286 m²/g. However, in the case of peach kernels, a rise in pyrolysis temperature from 700°C to 800°C decreased the volume of micropores and reduced the specific surface area. This effect could be a result of pore sintering or blockage by tar polymerization [9,43]. Nevertheless, peach kernels pyrolyzed at 700°C presented the highest surface area (349 m²/g).

In the case of steam activation, Table **4** shows that at 700°C, specific surface area and microporosity of samples were drastically enhanced, with respect to pyrolyzed materials, by 1.4 to 3.8 fold. An increase in temperature to 800°C favoured a further increase in surface area (by 7 to 92%) and micropore structure, whereas an enlargement of mesopores width. Almond kernels presented the highest specific surface area, 1256.8 m²/g, followed by peach kernels 778 m²/g and walnut husks 692.8 m²/g. Similar or lower values were reported for almond shells, 1234 m²/g [44] and 601 m²/g [32], whereas somehow higher for walnut shells,

792 m²/g [32]. The volume of micropores was in the same range. On the other hand, when pyrolyzed biochars were activated with carbon dioxide at a high temperature, microporosity was developed, also confirmed by other studies [9-12,45,46], average pore size was reduced, and specific surface area increased by 1.8 to 3 fold. In comparison to steam activation, carbon dioxide presented a lower gasification reactivity, which resulted in a lower pore volume and consequently up to 2 fold decrease in specific surface area. The highest specific surface area under carbon dioxide atmosphere was obtained for walnut husks 637 m²/g, followed by almond kernels 607.6 m²/g and peach kernels 531 m²/g. In the case of walnut shells, some authors reported that if they are both physically and chemically activated by CO_2 and KOH, their specific surface area could reach 2305 m²/g [47,48].

The improvement of surface area and favouring of mesopores by steam against carbon dioxide activation of a variety of chars, such as sugar cane bagasse, corn straw and barley straw, agrees with the results of previous investigations [8,9,45,49,50]. Figure **3** clearly shows that activated biochars under study could become materials with great adsorption potential of inorganic or organic pollutants. Considering the yield and surface area, biochars obtained after steam gasification at 700°C and carbon dioxide gasification at 800°C are prompt to be further investigated. A following study by the authors will include the feasibility of these biochars for the adsorption of various contaminants, as well as adsorption kinetics.
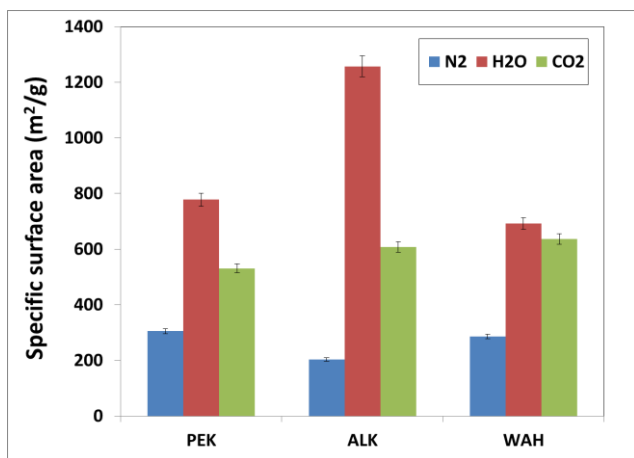
Figure 3: Specific surface area of biochars at 800°C.

3.4. Chemical Functional Groups of Pyrolyzed and Activated Biochars

The FTIR spectra of biochars obtained after steam or carbon dioxide activation at 800°C are represented in Figures **4** and **5**, respectively, and the chemical functional groups identified within the 400-4000 cm^{-1} wave number interval are summarized in Table **5**. These data show that gasified biochars at a high temperature were highly carbonized and exhibited highly aromatic structures.

In the case of steam activation, the bands in the range 800-900 cm^{-1} mainly represent aromatic C-H groups [9,12]. The sharp peaks at 1008, 1130 and 1210 cm^{-1} (Figure **4**) were associated with the C-O stretching vibration bands from ethers and alcohols [5,12,18]. Intense bands at 1420-1550 cm^{-1} are representative of C-H bending vibration, aromatic C=C functional groups, or –OH phenolic groups [5,9]. The band at 1630 cm^{-1}, corresponding to walnut husks, can be assigned to C=C stretching of aromatic components, while that at 1742 cm^{-1} corresponding to peach kernels to aromatic C-H stretching [5].

In the case of carbon dioxide activation, as seen in Figure **5**, the bands of ethers and alcohols C-O, aliphatic C-H, aromatic C=C, and phenolic –OH groups were sharper than in the presence of steam. Additionally, the peak of peach kernels at 2340 cm^{-1} is attributed to O=C=O stretching, while those in the range 2500-3000 cm^{-1}, appearing for all biochars, are ascribed to C-H deforming vibration mainly from aldehydes [5,9,11,18]. Finally, the broad bands, seen between 3000-4000 cm^{-1}, indicate the presence of hydroxyl groups –OH stretching from alcohols or phenols [5,9].

Overall, these results suggest that the absence of bands at 2500-3000 cm^{-1}, corresponding to aliphatic C-H groups and at 3000-4000 cm^{-1}, corresponding to –OH groups, during steam activation, indicate an increase in the aromaticity of chars, as compared to carbon dioxide activation. This has also been observed in other studies [9,12] for barley straw and corn straw biochars.
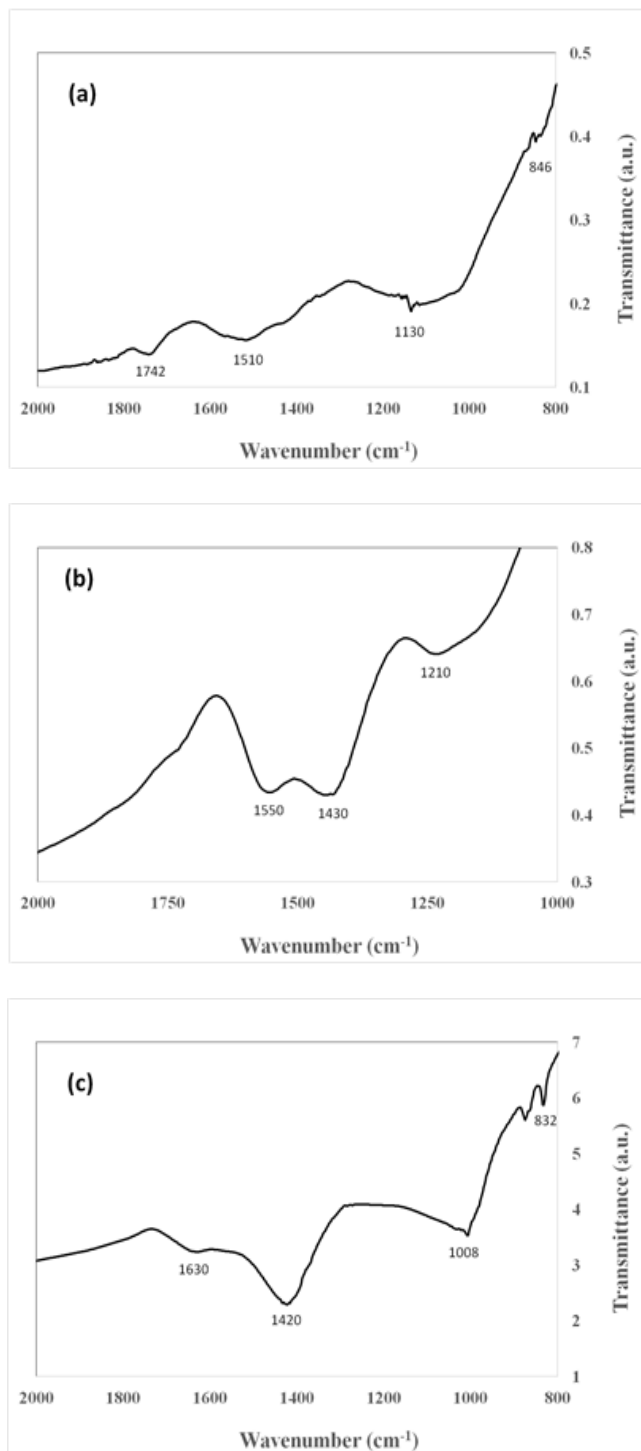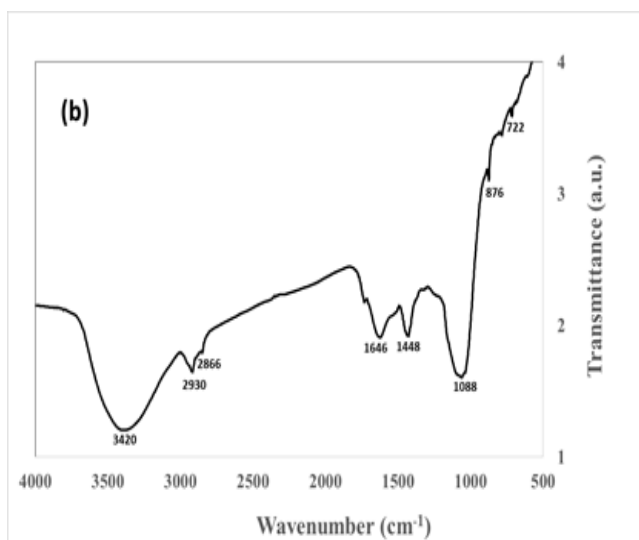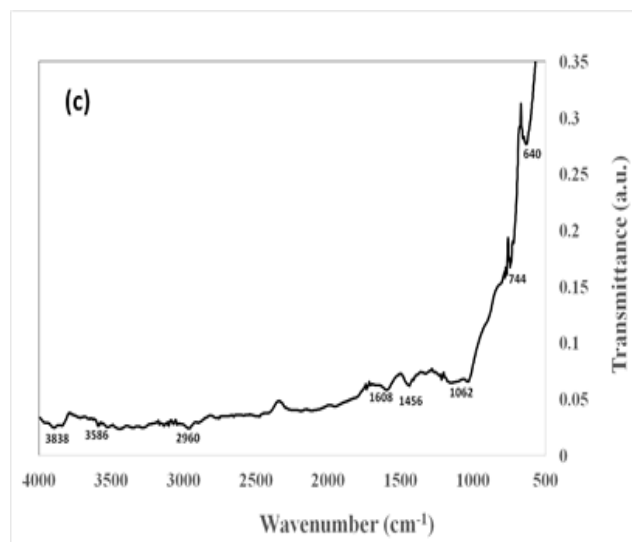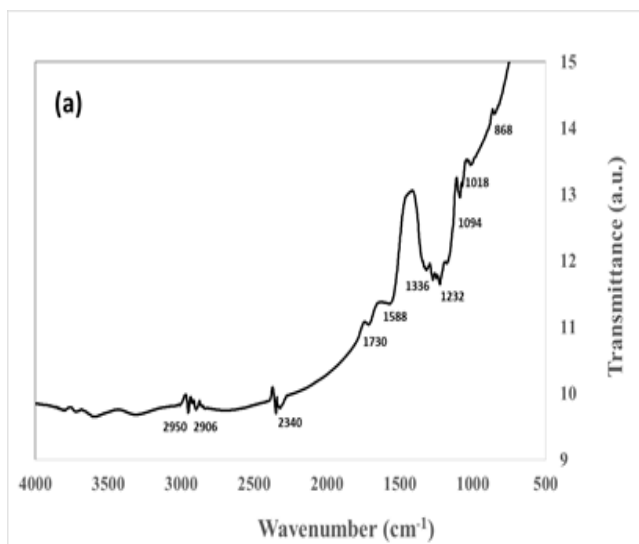

Figure 4: FTIR spectra of (a) peach kernels, (b) almond kernels, (c) walnut husks biochars activated by steam at 800°C.

Table 5:   FTIR Analysis of Biochars Activated by H_2O_v or CO_2

Wave Number (cm⁻¹)/Functional Groups	H_2Ov			CO_2		
	PEK	ALK	WAH	PEK	ALK	WAH
640-1000/C-H aromatic compounds	846		832/874	868	722/876	640/744
1000-1400/C-O alcohols, ethers	1130	1210	1008	1018/1094/1232	1088	1062
1300-1600/C-H alkanes, C=C aromatic compounds, -OH phenols	1510	1430/1550	1420	1336/1588	1448	1456
1600-1670/ C=C aromatic compounds			1630		1646	1608
1650-2000/ C-H aromatic compounds	1742			1730		
2000-2400/O=C=O carbon dioxide				2340		
2500-3000/C-H aldehydes				2906/2950	2866/2930	2960
3000-4000/-OH alcohols, phenols					3420	3586/3838

Figure 5: FTIR spectra of (a) peach kernels, (b) almond kernels, (c) walnut husks biochars activated by carbon dioxide at 800°C.

4. CONCLUSIONS

The combined pyrolysis-steam or –carbon dioxide gasification of nut residues of this study led to the production of a lower amount of biochars with respect to pyrolysis only and more syngas. A higher pyrolysis temperature resulted in an increase in the carbon density of biochars and a small enrichment in minerals. Activation by steam presented a higher reactivity than carbon dioxide, reduced the yield of biochars by 16-21%, consumed more oxygen organic functional groups, favoured pore enlargement at high temperature (24-31Å) and increased the specific surface area of pyrolyzed materials by 1.4 to 3.8 fold. Activation by carbon dioxide disrupted the hydrogen char structure, favoured microporosity, enhancing pore

volume by 76%, and increased the specific surface area of pyrolyzed materials by 1.8 to 3 fold. Gasified biochars at a high temperature were highly carbonized and exhibited aromatic structures, especially under steam activation. Activated biochars studied, with specific surface areas 693-1257 m^2/g under steam and 531-637 m^2/g under carbon dioxide, could become low-cost materials with great adsorption potential of hazardous species.

ACKNOWLEDGEMENT

REFERNCES

[1]   Wu R, Beutler J, Price C, Baxter L. Biomass char particle surface area and porosity dynamics during gasification. Fuel 2020; 264: 116833.
https://doi.org/10.1016/j.fuel.2019.116833

[2]   Panoutsou C. Bioenergy in Greece: Policies, diffusion framework and shakeholder interactions. Energ. Policy 2008; 36: 3674-3685.
https://doi.org/10.1016/j.enpol.2008.06.012

[3]   Yargicoglu E, Sadasivam BY, Reddy K, Spokas K. Physical and chemical characterization of waste wood derived biochars. Waste Manag. 2015; 36: 256-268.
https://doi.org/10.1016/j.wasman.2014.10.029

[4]   Genuino DA, De Luna MD, Capareda S. Improving the surface properties of municipal solid waste-derived pyrolysis biochar by chemical and thermal activation: Optimization of process parameters and environmental application. Waste Manag. 2018; 72: 255-264.
https://doi.org/10.1016/j.wasman.2017.11.038

[5]   Vamvuka D, Dermitzakis S, Pentari D. Valorization of Meat and Bone Meal through Pyrolysis for Soil Amendment or Lead Adsorption from Wastewaters. Food Bioprod. Process. 2018; 109: 148-157.
https://doi.org/10.1016/j.fbp.2018.04.002

[6]   Vamvuka D, Sfakiotakis S, Pantelaki O. Evaluation of gaseous and solid products from the pyrolysis of waste biomass blends for energetic and environmental applications. Fuel 2019; 236: 574-582.
https://doi.org/10.1016/j.fuel.2018.08.145

[7]   Sfakiotakis S, Vamvuka D. Thermal decomposition behaviour, characterization and evaluation of pyrolysis products of agricultural wastes. J. Energy Inst. 2017; 91: 951-961.
https://doi.org/10.1016/j.joei.2017.09.001

[8]   Hass A, Lima I. Effect of feed source and pyrolysis conditions on properties and metal sorption by sugarcane biochar. Environ. Techn. Innov. 2018; 10: 16-26.
https://doi.org/10.1016/j.eti.2018.01.007

[9]   Pallares J, Gonzalez-Cencerrado A, Arauzo I. Production and characterization of activated carbon from barley straw by physical activation with carbon dioxide and steam. Biomass

Bioenergy 2018; 115: 64-73.
https://doi.org/10.1016/j.biombioe.2018.04.015

[10]   Liu Z, Zhang F, Liu H, Ba F, Yan S, Hu J. Pyrolysis/gasification of pine sawdust biomass briquettes under carbon dioxide atmosphere: Study on carbon dioxide reduction and biochar briquettes physicochemical properties. Biores. Technol. 2018; 249: 983-991.
https://doi.org/10.1016/j.biortech.2017.11.012

[11]   Eshun J, Wang L, Ansah E, Shahbazi A, Schimmel K, Kabadi V. et.al. Characterization of the physicochemical and structural evolution of biomass particles during combined pyrolysis and CO2 gasification. J. Energ. Inst. 2019; 92: 82-93.
https://doi.org/10.1016/j.joei.2017.11.003

[12]   Xu M, Wu Y, Nan D, Lu Q, Yang Y. Effects of gaseous agents on the evolution of char physical and chemical structures during biomass gasification. Biores. Technol. 2019; 292: 121994.
https://doi.org/10.1016/j.biortech.2019.121994

[13]   Yu T, Abudukeranmu A, Anniwaer A, Situmorang Y, Yoshida A, Hao X. et.al. Steam gasification of biochars derived from pruned apple branch with various pyrolysis temperatures. Int. J. Hydr. Energ. 2020; 45: 18323.
https://doi.org/10.1016/j.ijhydene.2019.02.226

[14]   Koltowski M, Hilber I, Bucheli T, Charmas B, Skubiszewska-Zieba J, Oleszczuk P. Activated biochars reduce the exposure of polycyclic aromatic hydrocarbons in industrially contaminated soils. Chem. Eng. J. 2017; 310: 33-40.
https://doi.org/10.1016/j.cej.2016.10.065

[15]   Gong H., Tan Z., Zhang L., Huang Q. Preparation of biochar with high absorbability and its nutrient adsorption-desorption behaviour. Sci. Total Environ. 2019; 694:133728.
https://doi.org/10.1016/j.scitotenv.2019.133728

[16]   Vamvuka D, Sfakiotakis S. Gasification reactivity and mass spectrometric analysis of gases of energy crop chars under a CO2 atmosphere. Energy Fuels 2015; 29: 3215-3223.
https://doi.org/10.1021/acs.energyfuels.5b00376

[17]   Wang S, Gao B, Zimmerman A, Li Y, Ma L, Harris W, et.al. Physicochemical and sorptive properties of biochars derived from woody and herbaceous biomass. Chemosphere 2015; 134: 257-262.
https://doi.org/10.1016/j.chemosphere.2015.04.062

[18]   Onorevoli B, Pereira da Silva MG, Machado M, Corbelini V, Caramao E, Jacques R. Characterization of feedstock and biochar from energetic tobacco seed waste pyrolysis and potential application of biochar as an adsorbent. J. Environ. Chem. Eng. 2018; 6: 1279-1287.
https://doi.org/10.1016/j.jece.2018.01.039

[19]   Selvarajoo A, Oochit D. Effect of pyrolysis temperature on product yields of palm fibre and its biochar characteristics. Mater. Sci. Energ. Technol. 2020; 3: 575-583.
https://doi.org/10.1016/j.mset.2020.06.003

[20]   Bubba MD, Anichini B, Bakari Z, Bruzzoniti M, Camisa R, Caprini C. et.al. Physicochemical properties and sorption capacities of sawdust-based biochars and commercial activated carbons towards ethoxylated alkylphenols and their phenolic metabolites in effluent wastewater from a textile district. Sci. Total Environ. 2020; 708: 135217.
https://doi.org/10.1016/j.scitotenv.2019.135217

[21]   Hu Z, Vansant E. Synthesis and characterization of a controlled-micropore-size carbonaceous adsorbent produced from walnut shell. Micropor. Mater. 1995; 3: 603-612.
https://doi.org/10.1016/0927-6513(94)00067-6

[22] Aygun A, Yenisoy-Karakas S, Duman I. Production of granular activated carbon from fruit stones and nutshells and evaluation of their physical, chemical and adsorption properties. Micropor. Mesopor. Mater. 2003; 66: 189-195. https://doi.org/10.1016/j.micromeso.2003.08.028

[23] Martinez M, Torres M, Guzman C, Maestri D. Preparation and characteristics of activated carbon from olive stones and walnut shells. Ind. Crops Prod. 2006; 23: 23-28. https://doi.org/10.1016/j.indcrop.2005.03.001

[24] Mandal S, Sarkar B, Igalavithana AD, Ok YS, Yang X, Lombi E, Bolan N. Mechanistic insights of 2,4-D sorption onto biochar: Influence of feedstock materials and biochar properties. Biores. Technol. 2017; 246: 160-167. https://doi.org/10.1016/j.biortech.2017.07.073

[25] Benedetti V, Cordioli E, Patuzzi F, Baratieri M. CO2 adsorption study on pure and chemically activated chars derived from commercial biomass gasifiers. J. CO2 Utiliz. 2019; 33: 46-54. https://doi.org/10.1016/j.jcou.2019.05.008

[26] Sullivan G, Prigmore R, Knight P, Godfrey A. Activated carbon biochar from municipal waste as a sorptive agent for the removal of polyaromatic hydrocarbons, phenols and petroleum based compounds in contaminated liquids. J. Environ. Manag. 2019; 251: 109551. https://doi.org/10.1016/j.jenvman.2019.109551

[27] Sigmund G, Huffer T, Hofmann T, Kah M. Biochar total surface area and total pore volume determined by N2 and CO2 physisorption are strongly influenced by degassing temperature. Sci. Total Environ. 2017; 580: 770-775. https://doi.org/10.1016/j.scitotenv.2016.12.023

[28] Lee XJ, Lee LY, Gan S, Thangalazhy-Gopakumar S, Ng HK. Biochar potential evaluation of palm oil wastes through slow pyrolysis: Thermochemical characterization and pyrolysis kinetic studies. Biores. Technol. 2017; 236: 155-163. https://doi.org/10.1016/j.biortech.2017.03.105

[29] Gopu C, Gao L, Volpe M, Fiori L, Goldfarb J. Valorizing municipal solid waste: Waste to energy and activated carbons for water treatment via pyrolysis. J. Anal. Appl. Pyrol. 2018; 133: 48-58.
https://doi.org/10.1016/j.jaap.2018.05.002

[30] Aworn A, Thiravetyan P, Nhbanpote W. Preparation and characteristics of agricultural waste activated carbon by physical activation having macro and mesopores. J. Anal. Appl. Pyrol. 2008; 82: 279-285. https://doi.org/10.1016/j.jaap.2008.04.007

[31] Bouchelta C, Medjram M, Bertrand O, Bellat J. Preparation and characterization of activated carbon from date stones by physical activation with steam. J. Anal. Appl. Pyrol. 2008; 82: 70-77.
https://doi.org/10.1016/j.jaap.2007.12.009

[32] Gonzalez J, Roman S, Encinar J, Martinez G. Pyrolysis of various biomass residues and char utilization for the production of activated carbons. J. Anal. Appl. Pyrol. 2009; 85: 134-141.
https://doi.org/10.1016/j.jaap.2008.11.035

[33] Demiral H, Demiral I, Karabacakoglu B, Tumsek F. Production of activated carbon from olive bagasse by physical activation. Chem. Eng. Res. Dev. 2011; 89: 206-213. https://doi.org/10.1016/j.cherd.2010.05.005

[34] Bhushan B, Nayak A, Kotnala S. Green synthesis of highly porous activated carbon from jackfruit peel: Effect of operating factors on its physic-chemical characteristics. Mater. Today: Proceed. 2020. https://doi.org/10.1016/j.matpr.2020.08.554

[35] Zhang H, Voroney RP, Price GW. Effects of temperature and processing conditions on biochar chemical properties and their influence on soil C and N transformations. Soil Biol. Biochem. 2015; 83: 19-28. https://doi.org/10.1016/j.soilbio.2015.01.006

[36] Chen D, Chen X, Sun J, Zheng Z, Fu K. Pyrolysis polygeneration of pine nut shell: Quality of pyrolysis products and study on the preparation of activated carbon from biochar. Biores. Technol. 2016; 216: 629-636. https://doi.org/10.1016/j.biortech.2016.05.107

[37] Bardestani R, Kaliaguine S. Steam activation and mild air oxidation of vacuum pyrolysis biochar. Biomass Bioenergy 2018; 108: 101-112. https://doi.org/10.1016/j.biombioe.2017.10.011

[38] Azargohar R, Dalai AK. Steam and KOH activation of biochar: Experimental and modelling studies. Micropor. Mesopor. Mater. 2008; 110: 413-421. https://doi.org/10.1016/j.micromeso.2007.06.047

[39] Stasi C, Alvira D, Greco G, Gonzalez B, Manya J. Physically activated wheat straw-derived biochar for biomass pyrolysis vapors upgrading with high resistance against coke deactivation. Fuel 2019; 255: 115807. https://doi.org/10.1016/j.fuel.2019.115807

[40] Vamvuka D. Biomass, bioenergy and the environment, Tziolas Publications: Salonica 2009.

[41] Sfakiotakis S. Study on the exploitation of agricultural, urban and industrial wastes of Crete for power production-Thermal and kinetic analyses, PhD dissertation, Technical University of Crete: Chania 2016.

[42] Gonzalez J, Ramiro A, Carmen M, Gonzalez-Garcia C, Ganan J, Encinar J et al. Pyrolysis of almond shells. Energy applications of fractions. Ind. Eng. Chem. Res. 2005; 44: 3003-3012. https://doi.org/10.1021/ie0490942

[43] Zielinska A, Oleszczuk P, Charmas B, Skubiszewska-Zieba J, Pasieczna S. Effect of sewage sludge properties on the biochar characteristics. J. Anal. Appl. Pyrol. 2015; 112: 201-213. https://doi.org/10.1016/j.jaap.2015.01.025

[44] Macias-Perez M, Bueno-Lopez A, Lillo-Rodenas M, Salinas-Martinez de Lecea C, Linares-Solano A. SO2 retention on CaO/activated carbon sorbents. Part II: effect of activated carbon support. Fuel 2008; 87: 2544-2550. https://doi.org/10.1016/j.fuel.2008.01.022

[45] Carrier M, Hardie A, Uras U., Gorgens J., Knoetze J. Production of char from vacuum pyrolysis of South-African sugar cane bagasse and its characterization as activated carbon and biochar. J. Anal. Appl. Pyrol. 2012; 96: 24-32. https://doi.org/10.1016/j.jaap.2012.02.016

[46] Wu R, Beutler J, Price C, Baxter L. Biomass char particle surface area and porosity dynamics during gasification. Fuel 2020; 264: 116833. https://doi.org/10.1016/j.fuel.2019.116833

[47] Nowicki P, Pietrzak R, Wachowska H. Sorption properties of active carbons obtained from walnut shells by chemical and physical activation. Catal. Today 2010; 150: 107-114. https://doi.org/10.1016/j.cattod.2009.11.009

[48] Nor N, Chung L, Teong L, Mohamed A. Synthesis of activated carbon from lignocellulosic biomass and its applications in air pollution control-a review. J. Environ. Chem. Eng. 2013; 1: 658-666.
https://doi.org/10.1016/j.jece.2013.09.017

[49] Shahkarami S, Azargohar R, Dalai A, Soltan J. Breakthrough CO2 adsorption in bio-based activated carbons. J. Environ.

Sci. 2015; 34: 68-76. https://doi.org/10.1016/j.jes.2015.03.008

[50] Rambabu N, Rao B, Surisetty V, Das U, Dalai A. Production, characterization and evaluation of activated carbons from de-oiled canola meal for environmental applications. Ind. Crops Prod. 2015; 65: 572-581.